Immunology Letters 276 (2025) 107070

Contents lists available at ScienceDirect

Immunology Letters

journal homepage: www.elsevier.com/locate/immlet

Anti-inflammatory potential of pre-formulated *Aloe vera* in mitigating allergen-induced airway responses in mice

Rabia Sare Yanikoglu [a,b], Rumeysa Hekimoglu [c], Mert Celikten [d], Ayca Yıldız Pekoz [e], Ali Osman Gurol [f,g], Mukaddes Esrefoglu [c], Nuriye Akev [h], Tuğba Yılmaz Ozden [h], Beyza Goncu [i,*]

[a] Istanbul University, Institute of Health Sciences, Department of Biochemistry, Istanbul, Türkiye
[b] Bezmialem University, Faculty of Pharmacy, Department of Biochemistry, Istanbul, Türkiye
[c] Bezmialem University, Faculty of Medicine, Department of Histology and Embryology, Istanbul, Türkiye
[d] Bezmialem University, Experimental Research Center, Istanbul, Türkiye
[e] Istanbul University, Faculty of Pharmacy, Department of Pharmaceutical Technology, Istanbul, Türkiye
[f] Istanbul University, Aziz Sancar Institute of Experimental Medicine, Department of Immunology, Istanbul, Türkiye
[g] Istanbul University, Diabetes Application, and Research Center, Istanbul, Türkiye
[h] Istanbul University, Faculty of Pharmacy, Department of Biochemistry, Istanbul, Türkiye
[i] Bezmialem University, Vocational School of Health Services, Department of Medical Services and Techniques, Istanbul, Türkiye

ARTICLE INFO

Keywords:
Allergen induced airway inflammation
Aloe vera
propylene glycol
HSAEC
THP-1
OVA

ABSTRACT

Aloe vera, known for its rich phytochemical content, has long been used in traditional medicine. This study aimed to enhance its anti-inflammatory and anti-allergic properties by formulating an intranasal Aloe vera gel with propylene glycol (PgAv) and assessing its efficacy through *in vitro* and *in vivo* models. *In vitro*, PgAv and Aloe vera gel (Av) were tested on LPS-induced HSAEC cells for mRNA expressions of *TNFα, IL6, IL1β*, and *IL5*. Co-culture experiments revealed PgAv reduced TNFα and increased IFNγ, promoting a T_H1-type response. *In vivo*, PgAv was administered intranasally to BALB/c mice with OVA-induced allergic airway inflammation model (AIAR). PgAv reduced mRNA expression of pro-inflammatory cytokines in bronchoalveolar lavage fluid (BAL), decreased TNFα and OVA-IgE levels in plasma, and attenuated eosinophil infiltration and lung inflammation. While PgAv increased IL6 levels, it concurrently reduced PGD2 levels, indicating a therapeutic effect via prostanoid synthesis pathways. PgAv demonstrated superior efficacy compared to Av in modulating inflammatory responses, enhancing T_H1 responses for immunological balance, and mitigating T_H2-mediated inflammation. These findings suggest PgAv as a promising treatment for allergic airway inflammation, warranting further investigation to clarify the underlying mechanisms.

1. Introduction

The genus Aloe, which belongs to the Xanthorrhoeaceae family, has more than 360 species worldwide. The medicinal use of *Aloe vera* (*A. vera* (L.) Burm. f.) dates back to ancient times [1]. The gel contains about 75 compounds such as anthrons, carbohydrates, proteins,

Abbreviations: AECB, Airway Epithelial Cell Basal Medium; AIAR, Allergic Airway Inflammation Response; APS, Aloe-polysaccharide; Av, Aloe vera gel; BAL, Bronchoalveolar Lavage; CARAS, Combined allergic rhinitis and asthma mouse model; DMSO, Dimethyl sulfoxide; EDTA, Ethylenediamine tetraacetic acid; EGF, Epidermal growth factor; EMA, European Medicines Agency; FBS, Fetal Bovine Serum; H&E, hemotoxin eosin; HaCaT, High sensitivity of human epidermal keratinocytes; HSAEC, Human Small Airway Epithelial Cell Medium; h, hours; IFNγ, Interferon gamma; IgE, Immunoglobulin E; IL, Interleukin; LPS, Lipopolysaccharide; LTB4, Leukotriene B4; LYM, Lymphocytes; MONO, Monocytes; MTT, 3-(4,5-dimethylthiazol-2-yl)-2,5-diphenyltetrazolium bromide; NF-κB, Nuclear factor kappa B OVA, Ovalbumin; PCL, Polycaprolactone; Pg, Propylene glycol; PgAv, pre-formulated Aloe vera gel; PGD2, Prostaglandin D2; PLGA, Poly(lactic-co-glycolic acid); PVA, Poly(vinyl alcohol); RBC, Red blood cell; RNA, Ribonucleic acid; RPMI 1640, Roswell Park Memorial Institute Medium; qRT-PCR, Quantitative Real Time Polymerase Chain Reaction; T3, Triiodothyronine; Th, T helper; THP-1, Human Leukemia Monocytic Cell; TNFα, Tumour Necrosis Factor alpha.

* Corresponding author at: Bezmialem Vakif University, Ilhan Varank Building, Ugur Mumcu, Muhsin Yazicioglu Caddesi 2115 Sok. No: 6, 34265 Sultangazi/Istanbul, Turkiye.
E-mail addresses: bsgoncu@gmail.com, bgoncu@bezmialem.edu.tr (B. Goncu).

https://doi.org/10.1016/j.imlet.2025.107070
Received 10 April 2025; Received in revised form 15 July 2025; Accepted 7 August 2025
Available online 11 August 2025

glycoproteins, amino acids, organic acids, saponins, glucomannans, enzymes, lipids, and vitamins [2,3]. Studies have revealed the pharmacological effects of these bioactive compounds. *A. vera* plant has been shown to have anti-inflammatory [4], anti-aging [5] wound healing [6,7], antioxidant [8], anticancer [9,10], cardio-protective [11], antidiabetic [12], laxative [13], antimicrobial [14], and immunomodulatory [15] effects. The dagger-shaped leaves are made of mainly two parts: The leaf skin or cortex, known as rind, and the inner parenchyma gel or pulp. The gel, which is constituted of 95% water with acemannans as the major constituent, is known to be responsible for the immunomodulatory effect of the plant [14]. In another study, it was reported that the aloin active ingredient in *A. vera* suppresses the NF-κB pathway [16].

A. vera gel exhibits a structural configuration analogous to a polymeric chain network. An increase in elastic modulus was observed as the temperature increased. A reduction in viscosity was observed with an increase in shear rate. The viscous structure of the gel represents a critical parameter in the formulation process. In a study, it was emphasized that in addition to the existing viscosity of *A. vera* gel, the ratio of other substances to be formulated is of great importance. Otherwise, the viscosity problem may have adverse consequences in formulation use [17].

Airway inflammation has been demonstrated to be a fundamental feature of asthma [18–21]. Typically, this involves a mucosal infiltrate comprising eosinophils [20], mast cells [19], and activated lymphocytes, which collectively contribute to structural alterations, including epithelial damage, subepithelial fibrosis, and smooth muscle hypertrophy [21]. Airway hyperresponsiveness and inflammatory cell infiltration occur in allergic asthma, which is characterized by allergen-induced airway inflammation or response [22,23]. IL4, IL5, and IL13, which are some T_H2 cytokines accompanying inflammation, provide IgE production of B cells inducing isotype change [24,25]. Eosinophils, another immune cell that plays a role in allergic inflammation, lead to the release of histamine, LTB4, TNFα, and IL13 from mast cells, another phase of inflammation. Many studies have been conducted to investigate the effect of *A. vera*, which has strong bioactive components, on allergic inflammation [26,27]. In one of these studies, it was reported that OVA-specific IgE and T_H2 cytokine levels decreased after oral administration of the formulation containing *A. vera* gel in mice with an ovalbumin (OVA) induced food allergy model [28].

This study aims to formulate and diversify the usable forms of the anti-inflammatory and anti-allergic properties of *A. vera*, which have been demonstrated *in vitro* on numerous occasions, with a more effective orientation. This study employed propylene glycol (Pg), a well-known and well-studied excipient with European Medicines Agency (EMA) approval, which is frequently used in pharmaceutical preparations with *A. vera* gel. Pg is employed as a moisturizer in topical formulations, a preservative in solutions, and a co-solvent in aerosols, oral solutions, and topical applications [29–31]. The viscosity of *A. vera* gel represents a significant obstacle to the inhalation and intranasal (i.n.) applications of the substance and thus limits the scope of such studies. Accordingly, in accordance with EMA standards, we selected Pg as a vehicle and combined it with *A. vera* gel in the ratio that we determined to facilitate i.n. administration. To substantiate the efficacy of this approach, we examined the allergen-induced airway response (AIAR) in both *in vitro* and *in vivo* settings. In this regard, the present study is a preliminary step towards the preclinical phase.

2. Material and methods

2.1. In vitro

2.1.1. A. vera gel (Av) extraction

The *A. vera* plant specimen used in our study is registered in Istanbul University, Faculty of Pharmacy Herbarium (ISTE) with the number 65118 and cultivated in the Istanbul University Alfred Heilbronn Botanical Garden greenhouse. *A. vera* leaves were washed with distilled water and weighed. The leaves were left standing vertically in a beaker for one night to allow the brown latex rich in anthraquinones to flow and separate. The cut leaf parts were kept in the beaker for 1 night to separate the anthraquinones. The portion of the leaves kept in the beaker overnight was dissolved with distilled water and stored in the refrigerator at +4°C until use. The clear yellow gel was weighed, homogenized in a Waring Blender, and passed through a cloth filter.

2.1.2. Preparation of the pre-formulation of PgAV

To prepare pre-formulation, the Av was first subjected to lyophilization at 171 hPa for four days, with the conditions maintained at a temperature of -97°C. Subsequently, the pre-formulation (0.2%, w/v) was obtained by dissolving the lyophilized Av in a 20% (v/v) propylene glycol-PBS mixture. The ratio of propylene glycol and PBS was determined based on the viscosity of the gel. Viscosity assessment acquired from the Bezmialem Vakif University Drug Application and Research Center (ILMER) as a service purchase.

2.1.3. Cell culture

This study utilized two distinct cell lines: HSAEC (human primary small airway cells, PCS-301-010, ATCC) and THP-1 (human leukemia monocyte cell, TIB-202, ATCC). A specific basal media, designated as Airway Epithelial Cell Basal (AECB) medium, was prepared with the following components: HSA 500 μg/mL, linoleic acid 0.6 μM, lecithin 0.6 μg/mL, 6 mM L-glutamine, 0.4% Extract P, epinephrine 1.0 μM, and transferrin. The final insulin concentration was 10 nM, while that of triiodothyronine (T3) was 500 pM. Hydrocortisone, epidermal growth factor (EGF), and insulin were all present at 1 μg/mL. The penicillin concentration was 10,000 U/mL, while the streptomycin and amphotericin B concentrations were 10 mg/mL and 25 μg/mL, respectively. The THP-1 cells are suspension cells, and the recommended culture medium is RPMI 1640, which contains 10% FBS, 100 IU/mL penicillin, and 100 μg/mL streptomycin at final concentrations. At each passaging stage, trypsin/EDTA treatment was employed. The cells were then subjected to centrifugation, after which they were resuspended in fresh medium, and the passages were performed. Suitable cell stocks were cryopreserved between passages with DMSO at 5% (v/v) for HSAEC and 10% (v/v) for THP-1. *In vitro* cultivation processes were performed with cells frozen between passages 8 and 14 for HSAEC cell lines and between passages 3 and 6 for THP-1 cell lines.

In order to adapt the co-culture target medium, a transition to RPMI 1640 medium was undertaken. The HSAEC cell line was cultured in the target medium by applying gradual increases over three-weeks, with three passages occurring each week. The cells were cultured at a series of ratios, including 25%:75% (RPMI1640:AECB), 50%:50% (RPMI1640:AECB), 75%:25% (RPMI1640:AECB), and 100%:0% (RPMI1640:AECB), respectively. Both media contain 10% fetal bovine serum (FBS), 100 IU/mL penicillin, and 100 μg/mL streptomycin at final concentrations. Adaptation to the medium was monitored morphologically under a microscope.

2.1.4. Viability assessment

The tetrazolium salt 3-(4,5-dimethyl-2-thiazolyl)-2,5-diphenyl-2H-tetrazolium bromide (Thermo Fisher Scientific, NY, USA) is yellow and is easily incorporated by viable cells and reduced by the mitochondrial enzyme succinate dehydrogenase to the formazan compound, which is purple [32]. HSAEC cells were seeded in a 96-well plate (density of 5×10^3 cells per well) in a 5% CO_2 atmosphere for 24 h at 37°C. Then, the Av and PgAv were dispersed in airway epithelial cell basal medium with 10 concentrations (1000, 500, 250, 125, 62.5, 31.25, 15.62, 7.81, 3.9, and 1.95 μg/mL). Cells were incubated for 24 and 48 hours (h). The cells were washed with PBS three times to remove residual samples before injecting a fresh cell culture medium into the wells. The stock MTT solution was diluted at 1:10 with a cultivation medium (without phenol red and FBS), and the assay was performed as described previously [32]. The absorbance of the supernatant was measured at 570 nm. All

experiments were performed in triplicate/treatment. Statistical analyses were performed to compare the differences between viability and half-maximal inhibitory concentration values (IC_{50}). IC_{50} values were calculated using a four-parameter logistic regression model by a Quest Graph IC_{50} Calculator [33].

2.1.5. Total RNA isolation and cDNA synthesis

HSAEC cells were induced using one μg/mL LPS for 24 h [34], and an additional 24 h of treatment were performed with/without Av and PgAv following LPS-induction. All experiments were conducted in duplicate for each of the three independent experiments. Then, the total RNA was extracted using the EcoPURE Total RNA Kit (Ecotech, Erzurum, Türkiye). The final elution buffer volume was 30 μl. The concentration and quality of the isolated RNA were determined by measuring the 260/280 nm absorbance ratio using Multiscan Go (Thermo Fisher Scientific, MA, USA). Subsequently, the RNA concentration was adjusted to 10 ng/μL for each sample. Then, cDNA synthesis was conducted using a High-Capacity cDNA Reverse Transcription Kit (Applied Biosystems, MA, USA), per the manufacturer's instructions. The obtained cDNAs were stored at –20°C for further evaluation.

2.1.6. Evaluation of mRNA levels

A total of five genes were assessed, including *TNFα, IL5, IL6*, and *IL1β* mRNA expressions, and human *ACTB* (beta-actin; cytoskeletal structural protein) was employed for relative mRNA expression analysis. Primer design for these genes was conducted using the Primer3Plus software [35]. The list of primers and annealing temperatures is presented in Table S1. The primer specificity was confirmed in silico using the UCSC database, followed by a BLAST search [36]. The optimal annealing temperature was identified through gradient PCR in a T100 Thermal Cycler (Bio-Rad, CA, USA), and the resulting products were quantified via agarose gel electrophoresis. All cDNA samples were diluted 1:5 with ultrapure water before further experiments. After that, the expression levels were evaluated with 2X SYBR Green Kit (Nepenthe Arastirma Teknolojileri, Türkiye) according to the manufacturer's instructions with the CFX Connect Real-Time PCR Detection System (Bio-Rad, CA, USA). Samples were tested as duplicates on the same 96-well PCR plate per sample in 40 cycles, and the mean Cq values were utilized for subsequent analysis. qRT-PCR was conducted using a two-step method, comprising a denaturing step at 95°C for 5 seconds, an annealing step for 15 seconds, an extension step at 72°C for 10 seconds, and a final extension step at 72°C for 2 minutes.

2.1.7. Determination of cytokine levels

Cytokine levels were assessed using sandwich ELISA kits for supernatant samples. All experiments were performed in triplicate across three independent experiments. TNFα and IFNγ levels were measured, and ELISA kits were purchased from Thermo Fisher Scientific. Recommended kit protocols were followed.

2.2. In vivo

2.2.1. Allergen-induced airway response model (AIAR)

This study was conducted after approval from the Local Animal Ethics Committee (approval number: 2019265). BALB/c mice were housed and fed *ad libitum* and randomly divided into the following groups: pre-op (n=6), sham group received Alum alone during the sensitization phase, without OVA. During the challenge phase, phosphate-buffered saline (PBS) was administered intranasally under the same anesthesia and procedural conditions. This group was included to control for the potential effects of the adjuvant and procedural manipulations in the absence of antigen exposure (n=6). After allergen-induced airway response (AIAR) model: post-model (n=6) and PgAv treatment groups (48 h, 96 h, 144 h treatment durations, n = 18; six per group). BALB/c mice aged 8-10 weeks were subjected to a 21-day airway inflammation response including two phases: sensitization and challenge [37,38] In the sensitization phase, the OVA+Alum mixture was prepared with final concentrations of 2 mg/kg for OVA and 80 mg/kg for Alum and administered intraperitoneally for seven days (Fig. S1). After a 10-day interval, OVA solution with a final concentration of 0.4 mg/mL was administered intranasally to each mouse slowly over a 15 minutes under general anesthesia. Mice were kept in a vertical position for at least one minute, and normal breathing was observed throughout the process. This procedure was repeated once a day for 4 days [38]. During the entire 21-day period, weights and feed consumption of the mice were monitored. Blood samples were collected from BALB/c mice in the submandibular region during the experimental phases. The collection of blood samples was conducted through the facial vein (vena facialis). No anesthesia was administered, and a single puncture was made in the submandibular triangle, then blood samples were collected and hemogram measurement was performed instantaneously with 1/10 of the blood. Remaining blood is collected into green-capped (heparinized) pediatric tubes. Approximately 100–200 μL of blood was obtained from each mouse, and bleeding was stopped by applying short-term pressure. The samples were centrifuged, and plasma samples were stored at -80°C until further experimentation.

2.2.2. PgAv treatment

The concentration of the pre-formulation (PgAv) administered per mouse was calculated based on body surface area [39]. Based on the data obtained from *in vitro* experiments, the therapeutic concentration of PgAv was administered intranasally at 7.8 μg per 40 μl with limited sedation (inhalant agent), slowly, under breathing monitoring. The PgAv treatment phase was administered every 24 h. The 48, 96, and 144 h treatments included two, four, and six i.n. administrations respectively and are referred to as 48 h, 96 h, and 144 h throughout the text.

2.2.3. BAL fluid mRNA levels

Retrieved BAL fluids were centrifuged at 500 g for 3 min. Then, total RNA isolation was performed from BAL fluids using the EcoPURE Total RNA Kit. The process of cDNA synthesis was carried out using the same kit utilized in the *in vitro* stage. qRT-PCR carried out for five genes including mouse *IL1β, TNFα, IL5, IL6, IFNγ, IL4* and *RPLP0* (ribosomal protein, large, P0; synonym 36B4) was utilized as a reference gene. Optimizations for the relevant primer melting temperature were completed by gradient PCR (Table S1). mRNA levels were determined by qRT-PCR, employing the aforementioned materials and methods in the *in vitro* section.

2.2.4. Histopathological analysis

The lung tissue samples were fixed in 10% neutral buffered formalin for 24 h. The fixed tissue samples were then processed using the routine light microscope tissue processing method, whereby they were dehydrated by passing through graded alcohols. Subsequently, the samples were embedded in paraffin after clearing in xylol. Sections 3 – 4 μm in thickness were excised from the paraffin blocks and mounted on positively charged slides using a rotary microtome. A series of decreasing alcohol concentrations was employed to rehydrate the slides following deparaffinization at 70°C. Meticulous staining with hematoxylin-eosin (H&E) was then conducted after rehydration. Finally, the slides were examined thoroughly and comprehensively under a light microscope (Nikon Eclipse 920248, U.S.A.). Each section was evaluated and scored considering the histopathological changes, including epithelial degeneration, cellular infiltration, hemorrhage, alveolar collapse, and septal thickening. Under 20X magnification, epithelial degeneration, cellular infiltration, hemorrhage, alveolar collapse, and septal thickening were scored separately in each section as: 0: absent; 1: Mild; 2: Moderate; 3: Severe, with a maximum score of 15. All histopathological assessments and scoring were blinded by two independent histopathologists (M.E. and E.R.H.) to ensure unbiased evaluation.

2.2.5. Plasma cytokine levels

Stored plasma samples were used for the TNFα, OVA-IgE, IL6, and PDG2 levels, which were determined by ELISA. TNFα and IL6 ELISA kits were purchased from Thermo Fisher Scientific, OVA-IgE and PDG2 from Cayman. The experimental procedures were executed following the manufacturer's protocol.

2.3. Statistical analysis

All data were normalized in relation to their respective controls and are presented as the mean ± standard error of the mean for each treatment group. All graphs and analyses were conducted using GraphPad Prism v10.3.1. $P < 0.05$ was considered sufficient to reject the null hypothesis, and asterisks represent different levels of significance; *$p < 0.05$, **$p < 0.01$, ***$p < 0.001$, and ****$p < 0.0001$. The Student's t-test (two-tailed) and/or Mann–Whitney U-tests were employed to ascertain the significance of the observed differences between the two groups when necessary, between time intervals or concentration groups. Comparisons among groups were performed using one-way analysis of variation (ANOVA) and/or two-way ANOVA with multiple comparison tests following Tukey's, Sidak's, and Dunnett's tests. The ratios of all 11 genes' relative mRNA expression levels for qRT-PCR were calculated with the $2^{\Delta\Delta ct}$ method [40]. In addition, ELISA data was calculated by using sigmoidal four-parameter logistic model.

3. Results

3.1. Viscosity assessment

The viscosity of the Av was determined to be 200 mPa.s using a rheometer. A pre-formulation was prepared by dissolving 0.2% (w/v) lyophilized Av and 20% (v/v) propylene glycol solution in PBS to achieve a suitable viscosity for the intended experiments. The viscosity values obtained for PgAv pre-formulation concentrations ranging from 62.5 to 1.95 μg/mL are presented in Table S4. The target viscosity range for further experiments (intranasal treatment) is 1–10 mPa·s [41,42].

3.2. Viability changes

We determined the working concentration using an MTT assay on HSAEC cells. Av and PgAv were compared with 10 different concentrations using two time intervals (24h and 48h). The adjusted viability changes were not significant but showed a concentration-dependent decrease for Av for both time intervals, except for the lowest concentrations at 1.98 and 3.96 μl/mL (p=0.0397 and p=0.0255, respectively) (Fig. 1A left graph). For PgAv, a similar decrease according to concentration gradient was determined between 1.98 and 62.5 μl/mL concentrations (for 1.98 p=0.0272, for 3.9 p=0.0329, for 7.8 p=0.0155, for 15.9 p=0.0345, for 31.7 p=0.0271, for 62.5 p=0.0235), and treatment with higher than those concentrations showed increased viability at 125 to 500 μl/mL when compared with untreated (for 125 p=0.0089, for 250 μl/mL p=0.0419, for 500 and 1000 μl/mL was not found significant) (Fig. 1A right graph). These differences resulted primarily from Av viscosity, and while using PgAv, Pg provided more support for Av to enhance the cultivation process with increased solubility. Furthermore, IC_{50} were determined for HSAEC cells. For Av, the IC_{50} value was 1033 μg/ mL for 24 h and 121 μg/mL for 48 h. The IC_{50} of PgAv value was 312 μg/mL for 24 h and increased to 500 μg/mL for 48 h. This result demonstrated is a reverse correlation between Av and PgAv through time. The most important factor is the high viscosity of the Av. Again, the increased solubility and viability over time due to the addition of Pg exhibit a comparable pattern to PgAv viability. Candidate treatment concentrations were determined at 3.9 μg/mL and 7.8 μg/mL for further assays.

3.3. Concentration-dependent modulation of pro-inflammatory cytokine expression by Av and PgAv in LPS-treated HSAEC cells

HSAEC cells were treated with Av and PgAv at 3.9 and 7.8 μg/mL concentrations for 24 h, subsequently, total RNA isolation was performed. The spectrophotometric assessment of total RNA samples estimated A260/280 ratios with an average of 1.92 (min. 1.78 - max. 2.11). The average RNA concentrations were 137.5 ng/μl. qRT-PCR results showed that *TNFα* and *IL5* mRNA levels showed high levels of changes depending on the concentration gradient, in particular, 7.8 μl/mL concentration of the PgAv group presented a significant decrease compared to LPS-treated HSAEC cells (p=0.0122 and p=0.0414, respectively) (Fig. 1B, 1C). In addition, after treatment with only Av for both concentrations (3.9 and 7.8 μg/mL), the *TNFα* and *IL5* cytokine mRNA levels showed similar results (p=0.068 for TNFα, and p=0.0287 for *IL5*). In Av treatment, *IL6* mRNA levels decreased for both concentrations (3.9 and 7.8 μg/mL) (p=0.0068). However, in LPS-treated Av and PgAv groups, *IL6* mRNA levels increased compared to untreated, while it also showed a decreasing pattern in the LPS-treated group. Statistically, only the 7.8 μg/mL concentration of the PgAv group was found to be significant (p=0.0122) (Fig. 1D). As expected, other pro-inflammatory cytokine *IL1β* mRNA levels showed a similar pattern to *IL6*, except only Av groups where lowest expression was seen (Fig. 1E). When compared with the LPS-treatment group, *IL1β* mRNA levels in the Av group for both candidate concentrations showed $2^{\Delta\Delta ct}$ ratios estimated as 0.0011 and 0.0036, the lowest levels among all cytokines (p=0.0068). Pro-inflammatory cytokines decreased more at the 7.8 μg/mL concentration than at the 3.9 μg/mL concentration; the effects were more pronounced at 7.8 μg/mL across all markers for the treatment target after LPS treatment. All standard deviations of mRNA relative expression results were compiled in Table S2.

3.4. In vitro co-culture model reveals differential modulation of TNFα and IFNγ levels by Av and PgAv in airway inflammation

Subsequently, we performed an *in vitro* airway inflammation response with direct cell contact co-culture to understand the process in more detail. Before to co-culture, the HSAEC and THP-1 cell lines were prepared for medium adaptation, based on literature, by stimulating THP-1 monocyte cells with LPS, at an induction concentration of 1 μg/mL for a 3 and 6 h. The HSAEC and THP-1 cell lines were co-cultured at a ratio of 1:10 (THP-1:HSAEC) as previously reported [43] and treated with Av and PgAv at 3.9 and 7.8 μg/mL concentrations (Fig. 1F). After 24 h of treatment, the supernatants were collected and analyzed for TNFα and IFNγ levels. PgAv treatment resulted in an elevation of TNFα levels following both 3 and 6 h LPS induction periods. Specifically, at a 3.9 μg/mL concentration, TNFα levels significantly increased after 3 h of LPS stimulation (p = 0.0192) (Fig. 1G, upper panel). Concurrently, IFNγ levels also showed a significant increase in the PgAv-treated groups, particularly at both LPS induction time points, with the most pronounced effect observed at 3.9 μg/mL (p = 0.0002) (Fig. 1G, lower panel). Moreover, a comparison based on LPS stimulation durations revealed a significant positive correlation (p = 0.0056). All standard deviations of cytokine measurements are provided in Table S3.

3.5. Dynamic hematological and physiological outcomes in an AIAR treated with PgAv

A total of 27 days of experimental flow, including 21 days of model creation and treatment of mice, was completed (Fig. 2A). Throughout this process, the weights, feed consumption and hemogram parameters of the animals were monitored on a weekly basis during the pre-op, sensitization, and challenge stages (Fig S2). Following the establishment of the mouse model, the sham groups exhibited an increase in weight over time, whereas the treatment groups demonstrated a weight stabilization. The evaluation of feed intake in the mice revealed a

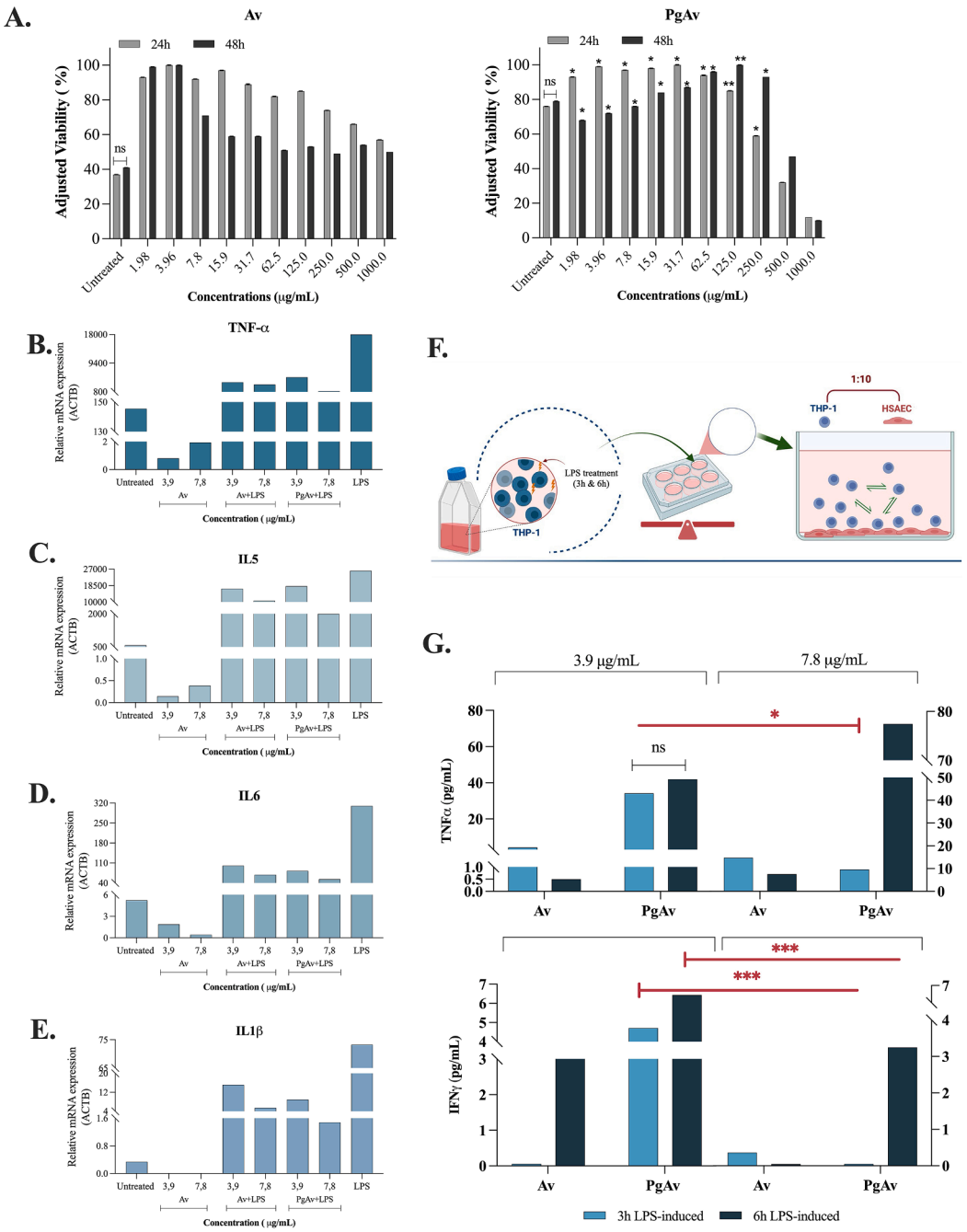

Fig. 1. Effect of PgAv on cytokine modulation and cell viability in *in vitro* and co-culture studies (A) Viability of HSAEC cells treated with Av and PgAv for 24 h and 48 h. MTT assay showed a mild concentration-dependent decrease in viability with Av, significant only at 1.98 and 3.96 µg/mL ($p = 0.0397$, $p = 0.0255$). PgAv induced a similar decrease between 1.98–62.5 µg/mL ($p < 0.05$ for all), but higher concentrations (125–250 µg/mL) increased viability ($p = 0.0089$, $p = 0.0419$). Differences were attributed to Av viscosity, with Pg improving solubility and cell compatibility. **(B-E)** Concentration-dependent effects of Av and PgAv on pro-inflammatory cytokine expression in LPS-treated HSAEC cells. HSAEC cells were treated with 3.9 and 7.8 µg/mL of Av and PgAv for 24 h. qRT-PCR analysis revealed that PgAv at 7.8 µg/mL significantly reduced *TNFα* and *IL5* expression compared to the LPS group ($p = 0.0122$, $p = 0.0414$). Av treatment showed similar trends, with significant *IL5* reduction ($p = 0.0287$) and borderline *TNFα* change ($p = 0.068$). *IL6* levels decreased with Av in both doses ($p = 0.0068$), whereas PgAv reduced *IL6* significantly only at 7.8 µg/mL ($p = 0.0122$). *IL1β* expression followed a similar pattern. **(F)** Schematic illustration of the co-culture experiment. **(G)** TNFα and IFNγ levels in co-culture following PgAv treatment under different LPS induction periods. After 24 h of treatment, PgAv at 7.8 µg/mL caused a significant TNFα increase after 6 h LPS induction ($p = 0.0192$), while IFNγ levels significantly increased at 3.9 µg/mL across both induction periods ($p = 0.0002$). A time-dependent rise in IFNγ was also observed ($p = 0.0056$), suggesting differential cytokine modulation by PgAv prior to *in vivo* validation. Light blue bars indicate 3 h of LPS exposure and dark blue bars represent 6 h of LPS exposure. Av: Aloe vera gel; HSAEC: human small airway epithelial cell; LPS: lipopolysaccharide; MTT: 3-(4,5-dimethylthiazol-2-yl)-2,5-diphenyltetrazolium bromide; PgAv: pre-formulation prepared with Aloe vera gel and propylene glycol; THP-1: human leukemia monocytic cell; µg/mL: microgram per milliliter. *$p < 0.05$, **$p < 0.01$, ***$p < 0.001$.

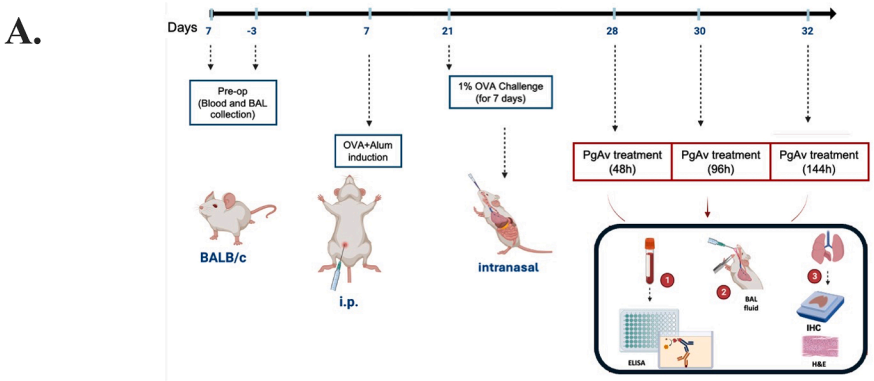

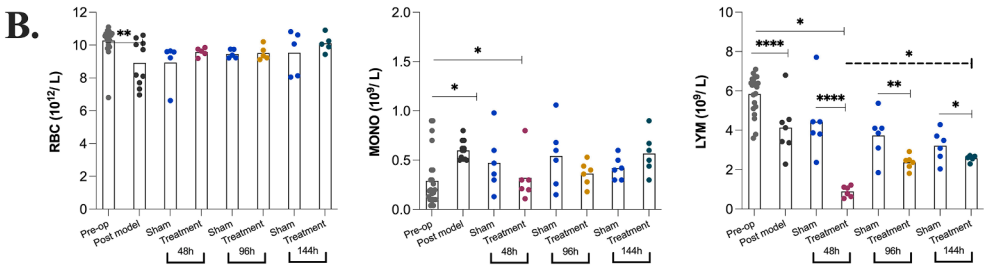

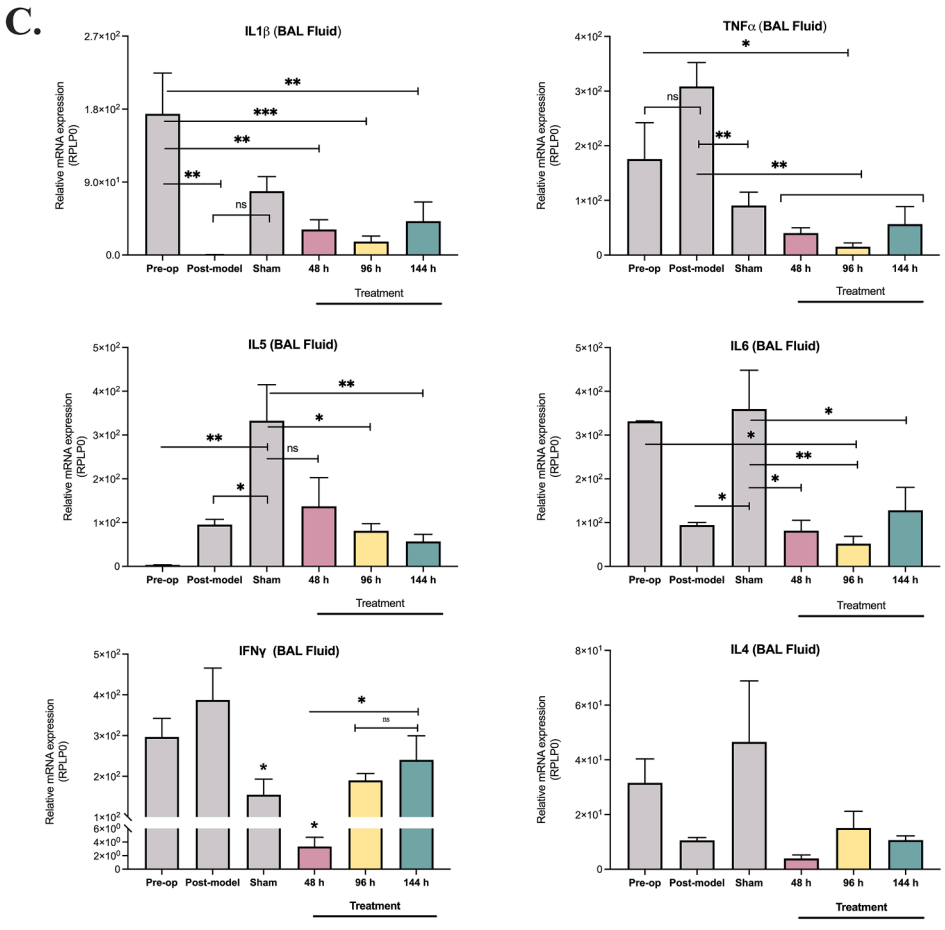

(caption on next page)

Fig. 2. Effect of PgAv on hematological and cytokine responsesin an allergen induced airway inflammation response model (AIAR). (A) Experimental scheme of AIAR model in BALB/c mice and PgAv administration timeline. **(B)** Hemogram analysis showing changes in RBC, MONO, and LYM counts during pre-op, post-model, sham, and treatment phases. A mild increase in RBC and MONO was observed post-PgAv treatment (MONO p = 0.0123); LYM count significantly increased from 48 h to 144 h (p = 0.0468). **(C)** mRNA expression levels of *IL1β, TNFα, IL5, IL6, IFNγ*, and *IL4* in BAL fluid assessed by qRT-PCR. PgAv significantly reduced pro-inflammatory cytokines at various timepoints (*IL1β* 96 h, p = 0.0007; *TNFα* 96 h, p = 0.0003; *IL5* 96 h, p = 0.0109; *IL6* 96 h, p = 0.0086; *IFNγ* 48 h to 144 h, p=0.0371; *IL4* ns for all h). *p<0.05, **p<0.01,***p<0.001, and ****p<0.0001. RBC: Red blood cells; MONO: Monocytes; LYM: Lymphocytes; BAL: Bronchoalveolar lavage.

decrease in consumption from the sensitization stage, which remained at consistent throughout the treatment. This outcome was positively correlated with the mice's weight change and developed due to the OVA/Alum induction process.

A decreased RBC count was observed from the pre-op to the post-model stage, with a declining profile. In the treatment groups, stability was observed following the post-model stage. While a slight increase was observed at 144h treatment in the RBC count and was not found statistically significant (Fig. 2B). The observed increase in RBC following treatment with PgAv provides evidence that the polysaccharides present in Av, as previously reported, possess erythropoiesis-stimulating properties [44]. Another parameter is the change in MONO levels. AIAR, which is known to have significant effects in the asthma model [45], increased in the treatment groups applied with PgAv (p=0.0123). The results demonstrate that the implemented model resulted in the predicted increase in inflammation. While the initial statistical analysis did not identify a significant difference at the outset of the treatment, subsequent observations revealed a fluctuating pattern. The observed decrease from pre-op to post-model stages is compatible with the sham group; however, LYM levels continued to increase during the treatment process. A statistically significant reduction was observed in all treatment groups compared to the pre-op (p < 0.0001 for all treatment groups). Noteworthy observation for LYM count showed a significant increase through 48h to 144 h treatment (p=0.0468) (Fig. 2B).

3.6. Temporal analysis of pro-inflammatory cytokine expression in BAL fluid following PgAv treatment in an AIAR model

The quality of RNA isolated from BAL samples revealed that all RNA samples exhibited A260/280 ratios with an average of 1.91 (minimum 1.77, maximum 2.05). The mean RNA concentration was 14.8 ng/μl (10.9–18.7 ng/μl). After treatment with PgAv, collected BAL fluids were used to assess relative mRNA expression levels of *IL1β, TNFα, IL5, IL6, IFNγ*, and *IL4* cytokines.

Upon examination of *IL1β* mRNA levels, a statistically significant decrease in expression levels was observed between pre-op and after AIAR (p=0.0008). *TNFα* mRNA expression levels between the pre-op and post-model groups, an increase in *TNFα* levels was observed, though this increase was not statistically significant (Fig. 2C). A significant difference was identified between the post-model and sham groups, with a notable decline in *TNFα* levels (p=0.0072). Similarly, a significant decrease was observed in the treatment process after the formation of AIAR (48 h, p=0.0013; 96 h, p=0.0003; 144 h, p=0.0010). Furthermore, the lowest level of *TNFα* was observed after 96 h of treatment, compared to the pre-op state (p=0.0417). Furthermore, a statistically significant increase was observed in *IL5* mRNA expression levels between the pre-op and sham groups (p=0.0035). Despite the absence of a statistically significant difference between the sham and post-model groups, an increase in *IL5* levels was observed. A decrease in *IL5* mRNA expression levels was noted when comparing the sham and two treatment groups (for 96 h, p=0.0109; for 144 h, p=0.0048) (Fig. 2C). An examination of the mRNA expression levels of another cytokine, *IL6*, revealed a decrease following the 96 h treatment period, when compared to the levels observed prior to the treatment (p=0.0469). With the formation of the AIAR, the levels of *IL6* increased (p=0.0497). As the treatment with PgAv continued, similar patterns were observed in *IL5* and *IL6* mRNA levels (48 h p=0.0196; 96 h p=0.0086; 144 h p=0.0352). Subsequently, when Similar to the *TNFα* and *IL6* levels, a decrease was also observed for treatment groups (48 h p=0.0031; 96 h p=0.0007; 144 h p=0.003) (Fig. 2C). *IFNγ* mRNA levels significantly declined in the post-model group compared to the sham group (p = 0.0412), as well as compared to the 48 h treatment group (p = 0.001). *IFNγ* expression was recovered throughout treatment, with levels increasing significantly from 48 to 144 h (p = 0.0371). This suggests that *IFNγ* is modulated in a biphasic manner, possibly in association with the immunomodulatory actions of PgAv. *IL4* mRNA expression exhibited group-dependent variability; however, none of the changes were statistically significant (Fig. 2C). A relative increase was observed in the sham group compared to the pre-op and post-model groups, but PgAv treatment did not significantly alter *IL4* expression levels. This finding suggests limited responsiveness of *IL4* to treatment under these experimental conditions.

3.7. Histopathological outcomes

Histopathological analysis of lung tissue sections revealed marked differences between experimental groups, highlighting the time-dependent therapeutic effects of PgAv in AIAR.

In the pre-op group, lung architecture appeared normal. Alveolar structures were well-organized with thin, homogeneous interalveolar septa, and no signs of inflammation, fibrosis, or epithelial degeneration. Bronchial and bronchiolar epithelial surfaces were intact, displaying no evidence of hyperplasia, dysplasia, or structural disruption (Fig. 3). In contrast, the post-model group showed pronounced histopathological damage. This included marked degeneration in bronchial and bronchiolar epithelium—evident as nuclear pyknosis, perinuclear and cytoplasmic edema, and epithelial cell death—resulting in significant accumulation of cellular debris within bronchiolar lumens (p = 0.0048). Additionally, widespread hemorrhage, thickened interalveolar septa, eosinophilic amorphous material accumulation, and dense inflammatory cell infiltration were observed, particularly around blood vessels and within the septal connective tissue.

In the PgAv 48 h treatment group, histopathological damage closely resembled the sham. Severe epithelial degeneration, lumen obstruction by cellular debris, thickened interalveolar septa, alveolar lumen collapse, hemorrhage, and inflammation were all evident. These findings suggest that early PgAv treatment alone was insufficient to reverse inflammation-induced tissue injury at this time point. Following 96 h of PgAv treatment, lung sections revealed considerable improvement. Although focal degeneration and alveolar collapse were still observed, the extent of hemorrhage and inflammation was markedly reduced. The mean hemorrhage score was significantly lower than that of the 48 h group (p = 0.0268), and many areas exhibited near-normal histological features.

After 144 h of treatment, a more pronounced reduction in pathological alterations was evident. Large regions of lung tissue appeared histologically healthy. While some areas still showed localized epithelial degeneration, septal thickening, and alveolar collapse, both epithelial degeneration scores (p = 0.0268, p = 0.0007 vs. sham and 48 h) and septal thickness scores (p = 0.0268 vs. 48 h) were significantly reduced, indicating progressive histological recovery over time (Fig. 3). These findings support the therapeutic potential of PgAv in modulating allergen-induced lung injury, with histological improvement becoming evident in a time-dependent manner.

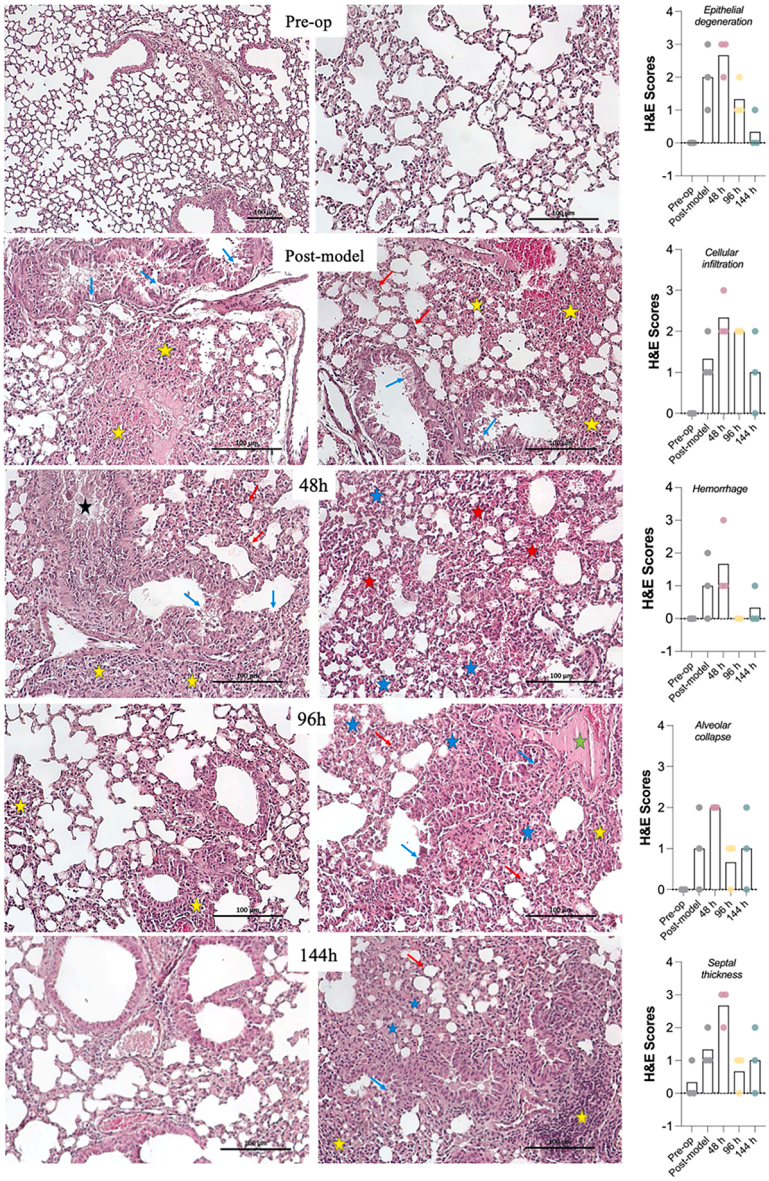

Fig. 3. Histopathological evaluation of lung tissue following PgAv treatment in the allergen-induced airway response (AIAR) model. Representative lung sections and histological scoring outcomes are presented for each experimental group. Upper left panel shows the pre-op group, corresponding to the healthy lung sections. Mid-left panel indicates the post-model; Lung sections exhibited marked degeneration in the bronchiolar epithelium, with epithelial cells and cellular debris visible in the lumen (blue arrows). The presence of hemorrhage, inflammatory cell infiltration (yellow asterisks), and thickening of interalveolar septa (red arrows) is observed. Upper right panel: lung sections from the PgAv 48 h treatment group exhibited significant degeneration in the epithelial lining of bronchiolar walls. This degeneration was characterized by epithelial cells and cellular debris visible within the lumen (blue arrows). The bronchiolar lumen, indicated by a black star, appears nearly completely obstructed by cellular debris. Hemorrhage, inflammatory cell infiltration (yellow asterisks), significant thickening of the interalveolar septa (red arrows), and alveolar lumen collapse (blue asterisks) are observed. The mid-right panel displays lung sections from the PgAv 96 h treatment group. A reduction in pathological changes is observed. In some regions of the lung, degeneration of the bronchiolar epithelium (blue arrows), thickening of the interalveolar septa (red arrows), alveolar lumen collapse (blue asterisks), small areas of hemorrhage, inflammatory cell infiltration (yellow asterisks), and accumulation of amorphous material (green asterisks) are evident lower-right panel: Lung sections from the PgAv 144 h treatment group. A significant reduction in pathological changes is observed. In some areas of the lung, degeneration of the bronchiolar epithelium (blue arrows), thickening of the interalveolar septa (red arrows), alveolar lumen collapse (blue asterisks), small hemorrhage, and inflammatory cell infiltration (yellow asterisks) are visibly evident. All sections are X20 unless otherwise indicated. The graph displays the histological scores of five histological parameters in the *in vivo* groups.

3.8. Systemic modulation of inflammatory cytokines, OVA-specific IgE, and PGD2 levels by PgAv treatment in an AIAR mouse model

Blood samples were collected from mice at specified intervals throughout the experimental procedure, including the creation of the AIAR and the subsequent treatment phase. The plasma was separated, and the cytokine levels were evaluated. As is known, the quantity of plasma from mice is limited. Accordingly, the present study was conducted with a limited number of cytokines due to the constraints imposed by the limited frequency of blood collection and amount of plasma through AIAR and the treatment process. Among the observed variables, TNFα levels demonstrated a marked increase, which was statistically significant as a consequence of post-sensitization ($p=0.014$). Similarly, a significant increase was observed following i.n. OVA administration (post-challenge) ($p=0.042$). In particular, TNFα levels demonstrated a notable decline during the 144 h treatment with PgAv,

with a p-value of 0.037. This decline resulted in TNFα levels closely approximating the levels observed during the sensitization phase (Fig. 4).

The most crucial marker in the formation of the AIAR and in demonstrating the efficacy of the treatment is OVA-IgE, and it levels increased with OVA+Alum and subsequent i.n. OVA administration during post-sensitization and challenge processes, respectively (p=0.0286). After generating an AIAR, OVA-specific IgE levels were decreased by PgAv treatment at indicated time intervals (48, 96, 144 h) (p=0.0145). In the post-challenge stage, OVA-specific IgE levels were still increased despite the treatment being administered only twice (48 h). As expected, higher IgE levels continued after challenge. Subsequently, administration of four treatments (96 h) resulted in a decrease compared to two treatments (48 h). It was close to the post-challenge level for IgE and, in addition, six repeated treatments (144 h) with PgAv showed continuous decrease (p=0.0069) (Fig. 4). Another pro-inflammatory cytokine, IL6, demonstrated a statistically significant increase following post-sensitization (p=0.0011). A decrease was observed in the subsequent i.n. OVA (post-challenge) (p=0.0779), yet an increase was noted over time with the treatment process (at 96 h p=0.0193 and at 144 h p=0.0259) (Fig. 4).

The effects of allergic inflammatory cytokines, which are localized in the airway mucosa by the current AIAR model, result in activating IgE-dependent pathways. The prediction of a treatment pathway through cytokines in the model created within the scope of the study is contingent upon the stages obtained thus far. It is established that PGD2, produced from prostaglandins in the mechanism of airway inflammation, plays a role in the activation of eosinophils, fibroblasts, smooth muscle cells, and T_H2-type cells [46]. The remaining plasma samples obtained from mice were evaluated for their PDG2 content (Fig. 4). PGD2 levels did not differ significantly between the groups (pre-op, post-sens, post-prov, 48 and 96 h of treatment). An increase was observed during the post-challenge period, which continued until the treatment group was administered twice ($p<0.05$). Furthermore, it was determined that PDG2 levels decreased at the end of 144 h, which was the longest period of treatment, compared to both pre-op and post-challenge (p=0.0146 and p=0.0097 respectively).

4. Discussion

A. vera has a long history of medicinal use due to its powerful phytochemicals, which have antioxidant, antiviral, immunomodulatory,

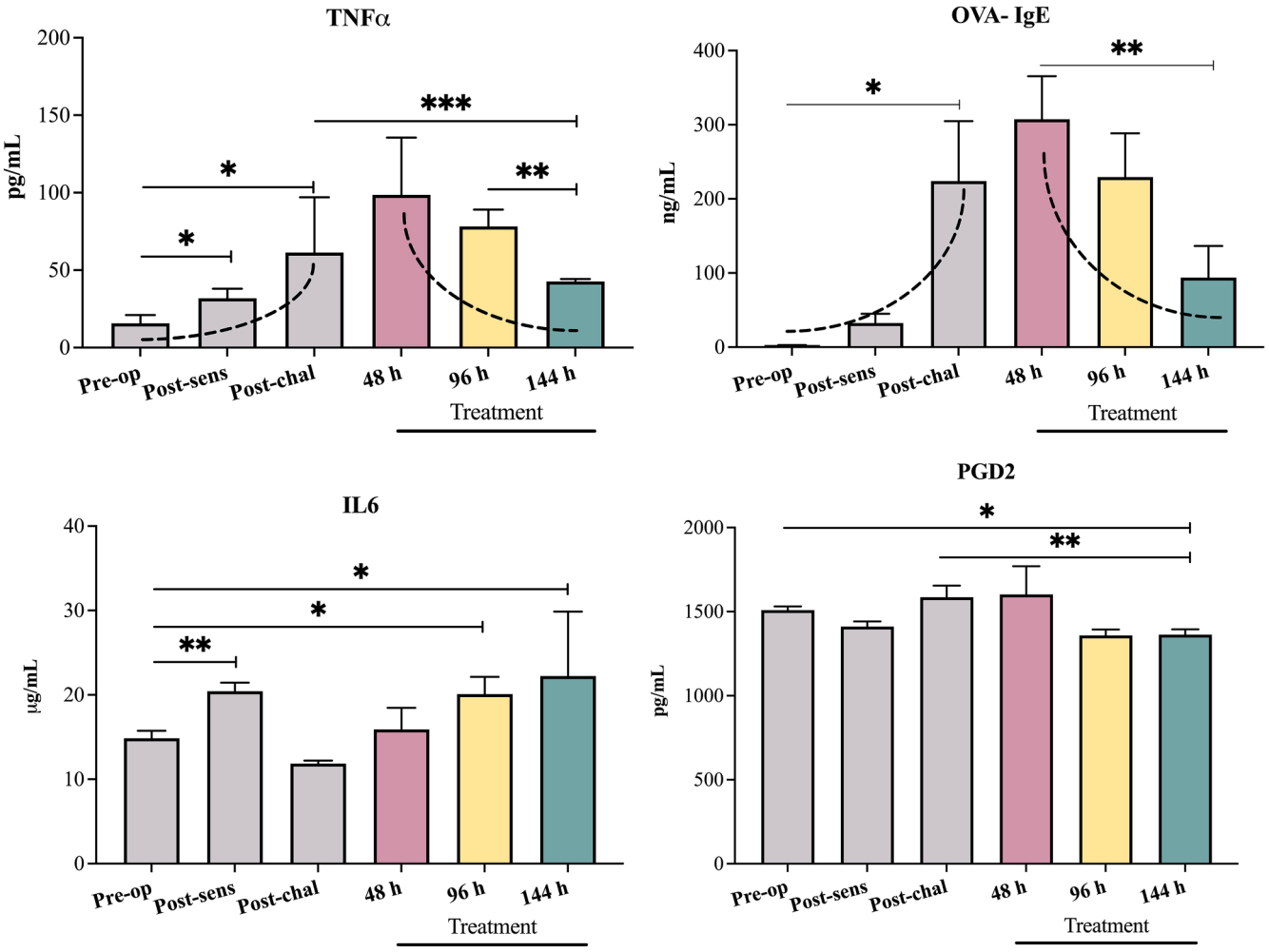

Fig. 4. Serum TNF-α, OVA-IgE, IL6 and PDG2 levels in mice were determined by ELISA. The serum levels of four inflammatory mediators (TNFα, OVA-IgE, IL6, and PGD2) were measured at different time points during the experimental protocol. The following time points were considered: pre-op, post-sens, post-chal, 48 h, 96 h, and 144 h post-treatment. TNFα: The levels of TNFα exhibit a significant increase following the sensitization and challenge phases. A peak is observed at 48 h post-treatment, gradually declining over time (96 h and 144 h). OVA-IgE: Serum levels of OVA-IgE display a marked increase following the challenge, with the highest levels being observed at 48 h post-treatment. As time progresses, the levels decrease gradually at 96 h and 144 h. IL6 levels progressively increase throughout the experimental phases, significantly rising at 144 h post-treatment. PGD2 levels remain relatively stable across the pre-op, post-sens, and post-chal phases but show a transient peak at 48 h post-treatment. The levels slightly decrease at 96 h and 144 h. Significant changes are noted with $p< 0.05$, $**p < 0.01$, and $***p < 0.001$. OVA: Ovalbumin; PDG2: prostaglandin D2.

and anti-inflammatory properties [47]. Although studies on allergic rhinitis and airway inflammation are limited, recent findings are promising. For instance, aloin, the active component of *A. vera,* thinned the nasal mucosa in the CARAS mouse model, reduced peribronchial inflammation, and decreased IL4, IL5, and IL13 levels in BALF [48]. Additionally, *A. vera* is frequently used in studies due to its cell regeneration properties [49]. Preformulations containing *A. vera* include polycaprolactone (PCL) [50–52], chitosan [53], poly(vinyl alcohol) (PVA) [54], and poly(lactic-co-glycolic acid) (PLGA) [55]. These formulations demonstrate the potential of *A. vera* in tissue engineering applications.

IgE-mediated allergic diseases, including asthma, allergic rhinitis, and atopic dermatitis, have been observed to demonstrate analogous inflammatory characteristics [56]. The distinguishing characteristics of these diseases are attributable to anatomical structure, inflammation levels, and interactions with airway smooth muscle cells, which result in symptoms such as bronchoconstriction or nasal congestion [57]. IgE-dependent mast cells, T_H2 cells, and ILC2 have been identified as the mediators of eosinophil infiltration [58]. In BALB/c mice, the i.n. delivery of the substance has been demonstrated to be more efficacious than the i.p. route at lower doses [59]. Furthermore, the probiotic Lactobacillus rhamnosus GG administered via the i.n. route has been shown to reduce airway hyperresponsiveness and IL5/IL13 levels [60]. The present findings suggest that the i.n. administration of the substance may constitute a viable alternative in cases of allergic airway inflammation.

We aimed to enhance the anti-inflammatory and anti-allergic effects of A. vera, previously shown *in vitro*. *A. vera* gel containing the EMA-approved Pg was selected as the preferred excipient. Subsequently, the LPS-induced inflammatory response pattern *in vitro* was determined in small airway epithelial cells. Both formulations preserved cell viability at low-to-moderate doses, but Av alone reduced viability over time, likely due to its viscosity and mucopolysaccharides. At >62.5 μg/mL, PgAv showed a nonlinear viability response, possibly due to Pg's nutrient-like or solubilizing effects. IC50 analysis further confirmed that both formulations had substantially higher IC50 values, supporting the use of lower concentrations for mechanistic studies. Working concentrations of 3.9 and 7.8 μg/mL were chosen to avoid off-target and cytotoxic effects. These doses fall within a range where moderate yet statistically significant changes in viability were observed and are well below the IC50 values. They also reflect a biologically relevant window that avoids artificial enhancement caused by higher solute levels. Thus, they were deemed appropriate for subsequent *in vitro* analyses.

Following stimulation with LPS in HSAEC cells, cytokine mRNA levels were evaluated after treatment with Av and PgAv. LPS increases the expression of proinflammatory cytokines, including *IL6, IL1β,* and *TNFα*, by binding to *TLR4* and activating the *NF-κB* pathway [61]. The study revealed consistent mRNA changes in *IL6, TNFα, IL1β*, and *IL5*. As demonstrated in previous studies [62,63], an increase in Av concentration has been shown to reduce *IL6* mRNA levels, and similar effects were observed in this study. It is evident that PgAv further strengthened this effect, providing a 25-fold decrease in *TNFα* mRNA levels compared to the untreated group. In addition, there was a 24-fold increase in *IL5*, a 9-fold decrease in *IL6*, and a 47-fold decrease in *IL1β*. The most significant discrepancy between the PgAv and Av groups indicated that the anti-inflammatory potential of PgAv was partially related to cytokine levels.

To assess potential *in vivo* effects, TNFα (pro-inflammatory) and IFNγ (inhibitory) levels were quantified in an LPS-induced co-culture inflammation model. Previous studies reported that peak NF-κB pathway activation and cytokine production in THP-1 cells occurred within 3–6 h post-LPS exposure [64,65]. Based on this, Av and PgAv were tested at different time points. Av treatment did not significantly affect TNFα levels, while PgAv showed a time-dependent effect: after 6 h of LPS exposure, TNFα levels declined, indicating a potential anti-inflammatory response. This suggests that PgAv may modulate TNFα expression depending on exposure duration, likely due to its bioactive components influencing signaling dynamics. Although PgAv demonstrated certain immunological effects at a dose of 7.8 μg/mL, we decided to use a 3.9 μg/mL concentration for *in vivo* studies based on both efficacy and consistency. Specifically, IFNγ levels increased significantly at 3.9 μg/mL under both short-term and long-term LPS induction, indicating that PgAv can reliably promote the T_H1-dominant immune response, indicating a reliable TH1-promoting effect and stable TNFα response. However, while some noticeable changes were observed at the 7.8 μg/mL concentration, these were generally inconsistent or paradoxical across different readings and conditions. Such variability raises reproducibility and therapeutic reliability concerns, particularly in more complex and dynamic *in vivo* environments. Therefore, 3.9 μg/mL was considered a more suitable candidate for further evaluation. We aimed to understand PgAv's mechanism rather than dose-response; hence, we prioritized reproducibility. This dose allowed precise evaluation of downstream mechanisms.

Various animal species have been used to study airway inflammation. Although rodents do not spontaneously develop asthma or allergy, their small size, low cost, and ease of sensitization make them preferable [66,67]. Discrepancies between human asthma and mouse models highlight the importance of selecting an appropriate model. According to Daubeuf's study, AIAR responses vary with an 8-day OVA induction. In another model, a 23-day induction reduced reproducibility due to repeated anesthesia for intranasal delivery [68]. Nevertheless, since a T_H2-directed immunologic response is obtained, the BALB/c and C57BL/6 mouse strains are predominantly utilized in related models. However, BALB/c mice are more frequently preferred than C57BL/6 mice due to their propensity to elicit a more robust T_H2-directed immune response [69,70]. We used female mice due to sex-based differences in airway inflammation. As demonstrated by Melgert et al. [71], female mice show a greater tendency to develop allergic airway inflammation and hyperresponsiveness compared to males. This makes female mice a more suitable and sensitive models.

To reduce bronchoconstriction-related AIAR and animal loss caused by varying intranasal OVA doses, a low dose of 0.4 mg/kg was chosen for the 21-day protocol [72]. After 21 days of AIAR, all groups maintained stable weights and showed reduced feed intake. Similar outcomes were assessed in an OVA-induced asthma model, which observed no adverse effects [73]. In our study, the stability of PgAv treatment in mouse weights was interpreted as an absence of side effects. A decrease in RBC count was seen from pre-op to post-model hemograms. RBC increase after PgAv supports the idea that Av polysaccharides may stimulate erythropoiesis [44]. MONO levels increase with inflammation. LYM levels decreased post-model as in the sham, then increased during treatment, with a later decline in prolonged treatments.

A comparison was conducted for mRNA expression levels of *IL1β, TNFα, IL5, IL6, IFNγ*, and *IL4* in BAL fluid samples to evaluate local rather than systemic effects further. As expected, *TNFα* mRNA levels increased with the progression of AIAR but declined upon PgAv treatment. Similarly, *IL6* levels decreased post-model and were further reduced with PgAv compared to sham and pre-op groups. The role of eosinophils in airway remodeling, mucus secretion, and T_H2-driven inflammation is well established [74], with activated eosinophils releasing cytokines such as *IL4, IL5, IL10*, and *IL13* [75,76]. In our model, *IL5* expression peaked in the sham group and declined progressively with PgAv, indicating a local anti-inflammatory effect. *IL1β* expression also declined from the pre-op to post-model phase, with lower levels observed in treatment groups than in sham. Notably, *IL1β* expression correlated positively with *IL6* levels. A time-dependent increase in *IFNγ* expression during treatment suggests potential immunomodulatory effects of PgAv. In contrast, *IL4* expression showed group-dependent variation without statistical significance, indicating limited responsiveness of *IL4* to PgAv under the current experimental conditions.

The alterations in BAL fluid mRNA expression profiles and lung

tissue histologic changes were examined concurrently. Airway inflammation, a hallmark of asthma, gives rise to structural alterations, encompassing epithelial damage, subepithelial fibrosis, and smooth muscle hypertrophy [21]. In the present study, the increased infiltration score of the post-model group was associated with increased scores of epithelial degeneration, alveolar collapse, septal thickening, and hemorrhage, as expected. The 48 h PgAv treatment group exhibited heightened alterations compared to the post-model group, while the 96 h treatment group demonstrated superiority in epithelial degeneration and cellular infiltration. Conversely, the 144 h treatment group exhibited optimal efficacy in controlling hemorrhage, alveolar collapse, and septal thickening. Except for the 48 h treatment group, the various treatment protocols positively impacted restoring healthy lung histology. The most challenging aspect of the study is determining the quantity of OVA-specific IgE and the impact of concomitant alterations in TNFα and IL6 levels on the treatment process. The limited plasma obtained from mice resulted in restricted cytokine evaluations.

Additionally, as is well established in the context of allergen-specific responses, there is an increase in the number of mast cells and activation of PDG2, which is influenced by the amount of arachidonic acid. Among the pathways potentially influenced by our pre-formulation, the process obtained with cytokines exhibited limited pathway specificity. Studies have shown that PGD_2 released peripherally can directly activate Th2 cells, increasing local IL4 and IL5 production without antigens or additional stimuli [77]. Alterations in mRNA expression in BAL fluid revealed increased *IL5* and decreased *TNFα, IL6*, and *IL1β* levels, indicating a predominant T_H2-type response rather than T_H1. This T_H2-directed profile suggests that IgE regulation may occur through alternative pathways, potentially modulated by PGD2-related mechanisms, particularly via mast cell activity. Supporting this, *IFNγ* expression exhibited a time-dependent increase during treatment, implying possible immunomodulatory effects of PgAv on T_H1-related responses. In contrast, *IL4* expression remained statistically unchanged across groups, indicating limited responsiveness to PgAv under the present experimental conditions.

In conclusion, our study underscores the potential of PgAv in managing allergic airway inflammation. By downregulating T_H2-associated cytokines and promoting a T_H1-related response, PgAv helps to correct the underlying immune imbalance characteristic of allergic conditions. Its ability to modulate key inflammatory pathways positions PgAv as a promising addition to current treatment strategies. Further studies are warranted to clarify the underlying signaling mechanisms, determine optimal dosing, and evaluate long-term efficacy.

Statement of ethics

Ethical approval for this study was obtained from Bezmialem Vakıf University Animal Research Center (DUAM) Ethical Committee (Approval Number/2019265). All animal experiments, The ARRIVE 2.0 guidelines and the National Research Council's Guide for the Care and Use of Laboratory Animals were carried out.

Funding

This study received financial support from the Scientific Research Projects Coordination Unit of Istanbul University (Project No. 36463) and Bezmialem Vakif University (Project No. 20221212).

CRediT authorship contribution statement

Rabia Sare Yanikoglu: Writing – original draft, Visualization, Project administration, Methodology, Formal analysis, Data curation, Conceptualization. **Rumeysa Hekimoglu:** Writing – original draft, Visualization, Methodology, Formal analysis, Data curation. **Mert Celikten:** Resources, Methodology. **Ayca Yıldız Pekoz:** Writing – review & editing, Methodology, Conceptualization. **Ali Osman Gurol:** Writing – review & editing, Writing – original draft, Methodology, Data curation, Conceptualization. **Mukaddes Esrefoglu:** Writing – original draft, Resources, Methodology, Conceptualization. **Nuriye Akev:** Writing – review & editing, Writing – original draft, Project administration, Methodology, Funding acquisition, Conceptualization. **Tuğba Yılmaz Ozden:** Writing – review & editing, Supervision, Methodology, Conceptualization. **Beyza Goncu:** Writing – review & editing, Writing – original draft, Supervision, Resources, Project administration, Methodology, Funding acquisition, Formal analysis, Conceptualization.

Declaration of competing interest

The authors declare the following financial interests/personal relationships which may be considered as potential competing interests:

Beyza Goncu reports financial support was provided by Bezmialem Vakif University. Nuriye Akev reports financial support was provided by Istanbul University. If there are other authors, they declare that they have no known competing financial interests or personal relationships that could have appeared to influence the work reported in this paper.

Acknowledgement

We would like to acknowledge the late Dr. Ozlem Akbal Dagistanli for their support in preparing the PgAv; her contributions were invaluable to this work. The authors gratefully acknowledge Professor Gulacti Topcu, Aydan Dag, Fahri Akbas, and Sezen Atasoy for their kind assistance and technical support regarding the provision of equipment.

Supplementary materials

Supplementary material associated with this article can be found, in the online version, at doi:10.1016/j.imlet.2025.107070.

References

[1] C.K. Sung, New Perspectives on Aloe, Springer US, 2006, https://doi.org/10.1007/0-387-34636-8.
[2] N. Akev, A. Can, N. Sütlüpınar, E. Çandöken, N. Özsoy, T.Y. Özden, R. Yanardağ, E. Üzen, Twenty years of research on Aloe vera, 2015.
[3] D. Hekmatpou, F. Mehrabi, K. Rahzani, A. Aminiyan, The effect of aloe vera clinical trials on prevention and healing of skin wound: a systematic review, Iran. J. Med. Sci. 44 (2019) 1–9.
[4] B. Vázquez, G. Avila, D. Segura, B. Escalante, Antiinflammatory activity of extracts from Aloe vera gel, J. Ethnopharmacol. 55 (1996) 69–75, https://doi.org/10.1016/S0378-8741(96)01476-6.
[5] F.A. Ahmed, T.A. El-Bassossy, A.A. Abdelgawad, A review: therapeutic, medicinal and food uses of aloe vera, Universal J. Pharmaceut. Res. (2024), https://doi.org/10.22270/ujpr.v8i6.1045.
[6] J.P. Heggers, A. Kucukcelebi, C.J. Stabenau, F. Ko, L.D. Broemeling, M.C. Robson, W.D. Winters, Wound healing effects of *Aloe* gel and other topical antibacterial agents on rat skin, Phytother. Res. 9 (1995) 455–457, https://doi.org/10.1002/ptr.2650090615.
[7] A. Surjushe, R. Vasani, D. Saple, Aloe vera: A short review, Indian J. Dermatol. 53 (2008) 163, https://doi.org/10.4103/0019-5154.44785.
[8] N. Ozsoy, E. Candoken, N. Akev, Implications for degenerative disorders: antioxidative activity, total phenols, flavonoids, ascorbic acid, β-carotene and β-tocopherol in *Aloe vera*, Oxid. Med. Cell Longev. 2 (2009) 99–106, https://doi.org/10.4161/oxim.2.2.8493.
[9] S.Erdem Kuruca, E. Çandöken, N. Akev, Investigation of aloe-emodin and Aloe vera gel extract on apoptosis dependent pathways in leukemia and lymphoma cell lines, Istanbul J. Pharmacy 1 (2020) 42–48.
[10] M. Mahyoob Alburyhi, A. El-Shaibany, M. Mahyoob Alburyhi, Formulation, development and evaluation of aloe vera extract capsules delivery system as an advanced phytotherapy approach for cancer *Corresponding Author, Research Article Alburyhi et al, World J. Pharmaceut. Res. 13 (2024) 1074, https://doi.org/10.20959/wjpr20248-32110. Www.Wjpr.Net. |.
[11] S. Sabbaghzadegan, H. Golsorkhi, M.H. Soltani, M. Kamalinejad, M. Bahrami, A. Kabir, M. Dadmehr, Potential protective effects of Aloe vera gel on cardiovascular diseases: A mini-review, Phytother. Res. 35 (2021) 6101–6113, https://doi.org/10.1002/ptr.7219.
[12] N. Ozsoy, R. Yanardag, A. Can, N. Akev, A. Okyar, Effectiveness of Aloe vera versus Glibenclamide on Serum Lipid Parameters, Heart and Skin Lipid Peroxidation in Type-II Diabetic Rats, 2008.

[13] S.K. Banyal, L. Bahadur, Aloes: a journey from traditional herb to modern panacea, Indian J. Tradit. Knowl. 23 (2024) 1055–1062, https://doi.org/10.56042/ijtk.v23i11.5019.
[14] M. Añibarro-Ortega, J. Pinela, L. Barros, A. Ćirić, S.P. Silva, E. Coelho, A. Mocan, R. C. Calhelha, M. Soković, M.A. Coimbra, I.C.F.R. Ferreira, Compositional Features and Bioactive Properties of Aloe vera Leaf (Fillet, Mucilage, and Rind) and Flower, Antioxidants 8 (2019) 444, https://doi.org/10.3390/antiox8100444.
[15] K. Imanishi, Aloctin A, an active substance of Aloe arborescens Miller as an immunomodulator, Phytother. Res. 7 (1993), https://doi.org/10.1002/ptr.2650070708.
[16] Y. Pengjam, H. Madhyastha, R. Madhyastha, Y. Yamaguchi, Y. Nakajima, M. Maruyama, NF-κB pathway inhibition by anthrocyclic glycoside aloin is key event in preventing osteoclastogenesis in RAW264.7 cells, Phytomedicine 23 (2016) 417–428, https://doi.org/10.1016/j.phymed.2016.01.006.
[17] A.W. Khan, J. Ali, S. Kotta, S.H. Ansari, R.K. Sharma, A. Kumar, Formulation development, optimization and evaluation of aloe vera gel for wound healing, Pharmacogn. Mag. 9 (2013) 6, https://doi.org/10.4103/0973-1296.117849.
[18] P.J. Barnes, A new approach to the treatment of asthma, N. Engl. J. Med. 321 (1989) 1517–1527, https://doi.org/10.1056/NEJM198911303212206.
[19] P.G. Gibson, C.J. Allen, J.P. Yang, B.J. Wong, J. Dolovich, J. Denburg, F. E. Hargreave, Intraepithelial mast cells in allergic and nonallergic asthma. Assessment using bronchial brushings, Am. Rev. Respir. Dis. 148 (1993) 80–86, https://doi.org/10.1164/ajrccm/148.1.80.
[20] J. Bousquet, P. Chanez, J.Y. Lacoste, G. Barnéon, N. Ghavanian, I. Enander, P. Venge, S. Ahlstedt, J. Simony-Lafontaine, P. Godard, Eosinophilic inflammation in asthma, N. Engl. J. Med. 323 (1990) 1033–1039, https://doi.org/10.1056/NEJM199010113231505.
[21] R. Djukanović, W.R. Roche, J.W. Wilson, C.R. Beasley, O.P. Twentyman, R. H. Howarth, S.T. Holgate, Mucosal inflammation in asthma, Am. Rev. Respir. Dis. 142 (1990) 434–457, https://doi.org/10.1164/ajrccm/142.2.434.
[22] J. Lötvall, C.A. Akdis, L.B. Bacharier, L. Bjermer, T.B. Casale, A. Custovic, R. F. Lemanske, A.J. Wardlaw, S.E. Wenzel, P.A. Greenberger, Asthma endotypes: a new approach to classification of disease entities within the asthma syndrome, J. Allergy Clin. Immunol. 127 (2011) 355–360, https://doi.org/10.1016/j.jaci.2010.11.037.
[23] G.M. Gauvreau, A.I. El-Gammal, P.M. O'Byrne, Allergen-induced airway responses, Eur. Respir. J. 46 (2015) 819–831, https://doi.org/10.1183/13993003.00536-2015.
[24] A. Bontinck, T. Maes, G. Joos, Asthma and air pollution: recent insights in pathogenesis and clinical implications, Curr. Opin. Pulm. Med. 26 (2020) 10–19, https://doi.org/10.1097/MCP.0000000000000644.
[25] Z.Celebi Sözener, L. Cevhertas, K. Nadeau, M. Akdis, C.A. Akdis, Environmental factors in epithelial barrier dysfunction, J. Allergy Clin. Immunol. 145 (2020) 1517–1528, https://doi.org/10.1016/j.jaci.2020.04.024.
[26] R.D. Herculano, T.O. Dos Santos, N.R. de Barros, G.S. Pegorin Brasil, M. Scontri, B. G. Carvalho, M. Mecwan, N. Farhadi, S. Kawakita, C.H. Perego, F.A. Carvalho, A. G. Dos Santos, N.B. Guerra, J.F. Floriano, C.U. Mussagy, Z. Tirpáková, D. Khorsandi, A. Peirsman, H.T. Nguyen, A. Gomez, K. Mandal, R.J. de Mendonça, B. Li, M.R. Dokmeci, V. Jucaud, Aloe vera-loaded natural rubber latex dressing as a potential complementary treatment for psoriasis, Int. J. Biol. Macromol. 242 (2023) 124779, https://doi.org/10.1016/j.ijbiomac.2023.124779.
[27] Y. Yang, J. Sun, H. You, Y. Sun, Y. Song, Z. Shen, T. Liu, D. Guan, Y. Zhou, S. Cheng, C. Wang, G. Yu, C. Zhu, Z. Tang, Aloe-emodin relieves allergic contact dermatitis pruritus by inhibiting mast cell degranulation, Immunol. Lett. 270 (2024) 106902, https://doi.org/10.1016/j.imlet.2024.106902.
[28] D. Lee, H.S. Kim, E. Shin, S.-G. Do, C.-K. Lee, Y.M. Kim, M.B. Lee, K.Y. Min, J. Koo, S.J. Kim, S.T. Nam, H.W. Kim, Y.H. Park, W.S. Choi, Polysaccharide isolated from Aloe vera gel suppresses ovalbumin-induced food allergy through inhibition of Th2 immunity in mice, Biomed. PharmacOther 101 (2018) 201–210, https://doi.org/10.1016/j.biopha.2018.02.061.
[29] European Medicines Agency, Propylene glycol used as an excipient. Report published in support of the 'Questions and answers on propylene glycol used as an excipient in medicinal products for human use' (EMA/CHMP/704195/2013), 2017.
[30] R.C. Rowe, P.J. Sheskey, S.C. Owen (Eds.), Handbook of pharmaceutical excipients, Handbook of pharmaceutical excipients, 5, Pharmaceutical Press, 2006.
[31] A.C. Williams, B.W. Barry, Penetration enhancers, Adv. Drug Deliv. Rev. 56 (2004) 603–618, https://doi.org/10.1016/j.addr.2003.10.025.
[32] B. Goncu, E. Sevgi, C. Kizilarslan Hancer, G. Gokay, N. Ozten, Differential anti-proliferative and apoptotic effects of lichen species on human prostate carcinoma cells, PLoS. One 15 (2020) e0238303, https://doi.org/10.1371/journal.pone.0238303.
[33] AAT Bioquest, AAT Bioquest, Inc. (2024, November 21). Quest GraphTM IC50 Calculator. AAT Bioquest., (2024).
[34] U. Grandel, D. Heygster, U. Sibelius, L. Fink, S. Sigel, W. Seeger, F. Grimminger, K. Hattar, Amplification of lipopolysaccharide-induced cytokine synthesis in non-small cell lung cancer/neutrophil cocultures, Mol. Cancer Res. 7 (2009) 1729–1735, https://doi.org/10.1158/1541-7786.MCR-09-0048.
[35] A. Untergasser, H. Nijveen, X. Rao, T. Bisseling, R. Geurts, J.A.M. Leunissen, Primer3Plus, an enhanced web interface to Primer3, Nucleic. Acids. Res. 35 (2007) W71–W74, https://doi.org/10.1093/nar/gkm306.
[36] S.F. Altschul, W. Gish, W. Miller, E.W. Myers, D.J. Lipman, Basic local alignment search tool, J. Mol. Biol. 215 (1990) 403–410, https://doi.org/10.1016/S0022-2836(05)80360-2.
[37] M. Casaro, V.R. Souza, F.A. Oliveira, C.M. Ferreira, OVA-Induced Allergic Airway Inflammation Mouse Model. Methods in Molecular Biology, Humana Press Inc., 2019, pp. 297–301, https://doi.org/10.1007/978-1-4939-8994-2_28.
[38] F. Daubeuf, N. Frossard, Performing Bronchoalveolar Lavage in the Mouse, Curr. Protoc. Mouse Biol. 2 (2012) 167–175, https://doi.org/10.1002/9780470942390.mo110201.
[39] M.C. Cheung, P.B. Spalding, J.C. Gutierrez, W. Balkan, N. Namias, L.G. Koniaris, T. A. Zimmers, Body Surface Area Prediction in Normal, Hypermuscular, and Obese Mice, J. Surg. Res. 153 (2009) 326–331, https://doi.org/10.1016/j.jss.2008.05.002.
[40] K.J. Livak, T.D. Schmittgen, Analysis of relative gene expression data using real-time quantitative PCR and the 2(-Delta Delta C(T)) Method, Methods 25 (2001) 402–408, https://doi.org/10.1006/meth.2001.1262.
[41] T. Furubayashi, D. Inoue, A. Kamaguchi, Y. Higashi, T. Sakane, Influence of formulation viscosity on drug absorption following nasal application in rats, Drug Metab. Pharmacokinet. 22 (2007) 206–211, https://doi.org/10.2133/dmpk.22.206.
[42] P.C. Pires, M. Rodrigues, G. Alves, A.O. Santos, Strategies to Improve Drug Strength in Nasal Preparations for Brain Delivery of Low Aqueous Solubility Drugs, Pharmaceutics. 14 (2022), https://doi.org/10.3390/pharmaceutics14030588.
[43] M. Keuper, A. Dzyakanchuk, K.E. Amrein, M. Wabitsch, P. Fischer-Posovszky, THP-1 Macrophages and SGBS Adipocytes - A New Human in vitro Model System of Inflamed Adipose Tissue, Front. Endocrinol. (Lausanne) 2 (2011) 89, https://doi.org/10.3389/fendo.2011.00089.
[44] A.A. Channa, I.H. Qazi, S.A. Soomro, A.H. Shah, J.A. Gandahi, R.A. Korejo, I.A. Shah, A. Kalhoro, B.-E.-A. Khaskeli, African Journal of Pharmacy and Pharmacology Effect of oral supplementation of Aloe vera extract on haematology indices and immune cells of blood in rabbit, 8 (2014) 497–501. https://doi.org/10.5897/AJPP2014.4018.
[45] S. Jiang, Q. Wang, Y. Wang, X. Song, Y. Zhang, Blockade of CCL2/CCR2 signaling pathway prevents inflammatory monocyte recruitment and attenuates OVA-Induced allergic asthma in mice, Immunol. Lett. 214 (2019) 30–36, https://doi.org/10.1016/j.imlet.2019.08.006.
[46] D.Elieh Ali Komi, L. Bjermer, Mast Cell-Mediated Orchestration of the Immune Responses in Human Allergic Asthma: Current Insights, Clin. Rev. Allergy Immunol. 56 (2019) 234–247, https://doi.org/10.1007/s12016-018-8720-1.
[47] Y. Gao, K.I. Kuok, Y. Jin, R. Wang, Biomedical applications of Aloe vera, Crit. Rev. Food Sci. Nutr. 59 (2019) S244–S256, https://doi.org/10.1080/10408398.2018.1496320.
[48] Y. Feng, H. Qiao, H. Liu, J. Wang, H. Tang, Exploration of the mechanism of aloin ameliorates of combined allergic rhinitis and asthma syndrome based on network pharmacology and experimental validation, Front. Pharmacol. 14 (2023) 1218030, https://doi.org/10.3389/fphar.2023.1218030.
[49] J.P. Heggers, R.P. Pelley, M.C. Robson, Beneficial effects of Aloe in wound healing, Phytother. Res. 7 (1993), https://doi.org/10.1002/ptr.2650070715.
[50] P. Carter, S.M. Rahman, N. Bhattarai, Facile fabrication of aloe vera containing PCL nanofibers for barrier membrane application, J. Biomater. Sci. Polym. Ed. 27 (2016) 692–708, https://doi.org/10.1080/09205063.2016.1152857.
[51] S. Suganya, J. Venugopal, S. Agnes Mary, S. Ramakrishna, B.S. Lakshmi, V.R. Giri Dev, Aloe vera incorporated biomimetic nanofibrous scaffold: a regenerative approach for skin tissue engineering, Iran. Polym. J. 23 (2014) 237–248, https://doi.org/10.1007/s13726-013-0219-2.
[52] R. Sridhar, S. Ravanan, J.R. Venugopal, S. Sundarrajan, D. Pliszka, S. Sivasubramanian, P. Gunasekaran, M. Prabhakaran, K. Madhaiyan, A. Sahayaraj, K.H.C. Lim, S. Ramakrishna, Curcumin- and natural extract-loaded nanofibres for potential treatment of lung and breast cancer: in vitro efficacy evaluation, J. Biomater. Sci. Polym. Ed. 25 (2014) 985–998, https://doi.org/10.1080/09205063.2014.917039.
[53] H. Adel Alawadi, K. Andarzbakhsh, A. Rastegari, Z. Mohammadi, M. Aghsami, F. Saadatpour, Chitosan-Aloe Vera Composition Loaded with Zinc Oxide Nanoparticles for Wound Healing: In Vitro and In Vivo Evaluations, IET. Nanobiotechnol. 2024 (2024) 6024411, https://doi.org/10.1049/2024/6024411.
[54] Q. Zhang, M. Zhang, T. Wang, X. Chen, Q. Li, X. Zhao, Preparation of aloe polysaccharide/honey/PVA composite hydrogel: Antibacterial activity and promoting wound healing, Int. J. Biol. Macromol. 211 (2022) 249–258, https://doi.org/10.1016/j.ijbiomac.2022.05.072.
[55] I. Garcia-Orue, G. Gainza, F.B. Gutierrez, J.J. Aguirre, C. Evora, J.L. Pedraz, R. M. Hernandez, A. Delgado, M. Igartua, Novel nanofibrous dressings containing rhEGF and Aloe vera for wound healing applications, Int. J. Pharm. 523 (2017) 556–566, https://doi.org/10.1016/j.ijpharm.2016.11.006.
[56] P.J. Barnes, Pathophysiology of allergic inflammation, Immunol. Rev. 242 (2011) 31–50, https://doi.org/10.1111/j.1600-065X.2011.01020.x.
[57] U. Sahiner, M. Akdis, A.C. Akdis, Introduction to Mechanisms of Allergic Diseases. Allergy Essentials, Elsevier, Armsterdam, 2022, pp. 1–25.
[58] A. Lei, Y. He, Q. Yang, X. Li, R. Li, Role of myeloid cells in the regulation of group 2 innate lymphoid cell-mediated allergic inflammation, Immunology 161 (2020) 18–24, https://doi.org/10.1111/imm.13232.
[59] Subhashini, P.S. Chauhan, S. Kumari, J.P. Kumar, R. Chawla, D. Dash, M. Singh, R. Singh, Intranasal curcumin and its evaluation in murine model of asthma, Int. Immunopharmacol. 17 (2013) 733–743, https://doi.org/10.1016/j.intimp.2013.08.008.
[60] I. Spacova, M.I. Petrova, A. Fremau, L. Pollaris, J. Vanoirbeek, J.L. Ceuppens, S. Seys, S. Lebeer, Intranasal administration of probiotic Lactobacillus rhamnosus GG prevents birch pollen-induced allergic asthma in a murine model, Allergy 74 (2019) 100–110, https://doi.org/10.1111/all.13502.

[61] J. Li, Y. Qin, Y. Chen, P. Zhao, X. Liu, H. Dong, W. Zheng, S. Feng, X. Mao, C. Li, Mechanisms of the lipopolysaccharide-induced inflammatory response in alveolar epithelial cell/macrophage co-culture, Exp. Ther. Med. 20 (2020) 76, https://doi.org/10.3892/etm.2020.9204.
[62] S. Salvi, A. Semper, A. Blomberg, J. Holloway, Z. Jaffar, A. Papi, L. Teran, R. Polosa, F. Kelly, T. Sandström, S. Holgate, A. Frew, Interleukin-5 production by human airway epithelial cells, Am. J. Respir. Cell Mol. Biol. 20 (1999) 984–991, https://doi.org/10.1165/ajrcmb.20.5.3463.
[63] P.R. Mills, R.J. Davies, J.L. Devalia, Airway epithelial cells, cytokines, and pollutants, Am. J. Respir. Crit. Care Med. 160 (1999) S38–S43, https://doi.org/10.1164/ajrccm.160.supplement_1.11.
[64] W. Chanput, J. Mes, R.A.M. Vreeburg, H.F.J. Savelkoul, H.J. Wichers, Transcription profiles of LPS-stimulated THP-1 monocytes and macrophages: a tool to study inflammation modulating effects of food-derived compounds, Food Funct. 1 (2010) 254, https://doi.org/10.1039/c0fo00113a.
[65] W. Chanput, J.J. Mes, H.J. Wichers, THP-1 cell line: An in vitro cell model for immune modulation approach, Int. Immunopharmacol. 23 (2014) 37–45, https://doi.org/10.1016/j.intimp.2014.08.002.
[66] C. Blume, D.E. Davies, In vitro and ex vivo models of human asthma, Eur. J. Pharm. Biopharm. 84 (2013) 394–400, https://doi.org/10.1016/j.ejpb.2012.12.014.
[67] A.T. Nials, S. Uddin, Mouse models of allergic asthma: acute and chronic allergen challenge, Dis. Model. Mech. 1 (2008) 213–220, https://doi.org/10.1242/dmm.000323.
[68] F. Daubeuf, N. Frossard, Acute Asthma Models to Ovalbumin in the Mouse, Curr. Protoc. Mouse Biol. 3 (2013) 31–37, https://doi.org/10.1002/9780470942390.mo120202.
[69] J.A. Boyce, K.F. Austen, No audible wheezing: nuggets and conundrums from mouse asthma models, J. Exp. Med. 201 (2005) 1869–1873, https://doi.org/10.1084/jem.20050584.
[70] M.L. Güler, J.D. Gorham, C.S. Hsieh, A.J. Mackey, R.G. Steen, W.F. Dietrich, K. M. Murphy, Genetic susceptibility to Leishmania: IL-12 responsiveness in TH1 cell development, Science 271 (1996) 984–987, https://doi.org/10.1126/science.271.5251.984.
[71] B.N. Melgert, D.S. Postma, I. Kuipers, M. Geerlings, M.A. Luinge, B.W.A. van der Strate, H.A.M. Kerstjens, W. Timens, M.N. Hylkema, Female mice are more susceptible to the development of allergic airway inflammation than male mice, Clin. Exp. Allergy 35 (2005) 1496–1503, https://doi.org/10.1111/j.1365-2222.2005.02362.x.
[72] V. Gasparik, F. Daubeuf, M. Hachet-Haas, F. Rohmer, P. Gizzi, J. Haiech, J.-L. Galzi, M. Hibert, D. Bonnet, N. Frossard, Prodrugs of a CXC Chemokine-12 (CXCL12) Neutraligand Prevent Inflammatory Reactions in an Asthma Model in Vivo, ACS. Med. Chem. Lett. 3 (2012) 10–14, https://doi.org/10.1021/ml200017d.
[73] B.G. Min, S.M. Park, Y.W. Choi, S.K. Ku, I.J. Cho, Y.W. Kim, S.H. Byun, C.A. Park, S. J. Park, M. Na, S.C. Kim, Effects of Pelargonium sidoides and Coptis Rhizoma 2 : 1 Mixed Formula (PS + CR) on Ovalbumin-Induced Asthma in Mice, Evid. Based. Complement. Alternat. Med. 2020 (2020) 9135637, https://doi.org/10.1155/2020/9135637.
[74] S.S. Possa, E.A. Leick, C.M. Prado, M.A. Martins, I.F.L.C. Tibério, Eosinophilic inflammation in allergic asthma, Front. Pharmacol. 4 (2013) 46, https://doi.org/10.3389/fphar.2013.00046.
[75] Q. Hamid, M. Tulic, Immunobiology of asthma, Annu. Rev. Physiol. 71 (2009) 489–507, https://doi.org/10.1146/annurev.physiol.010908.163200.
[76] H. Renz, C. Bachert, C. Berek, E. Hamelmann, F. Levi-Schaffer, U. Raap, H.-U. Simon, S. Ploetz, C. Taube, P. Valent, D. Voehringer, T. Werfel, N. Zhang, J. Ring, Physiology and pathology of eosinophils: Recent developments: Summary of the Focus Workshop Organized by DGAKI, Scand. J. Immunol. 93 (2021) e13032, https://doi.org/10.1111/sji.13032.
[77] L. Xue, S.L. Gyles, F.R. Wettey, L. Gazi, E. Townsend, M.G. Hunter, R. Pettipher, Prostaglandin D2 Causes Preferential Induction of Proinflammatory Th2 Cytokine Production through an Action on Chemoattractant Receptor-Like Molecule Expressed on Th2 Cells, J. Immunol. 175 (2005) 6531–6536, https://doi.org/10.4049/jimmunol.175.10.6531.